



Technical success rates and reliability of spin-echo echo-planar imaging (SE-EPI) MR elastography in patients with chronic liver disease or liver cirrhosis

Sang Lim Choi¹ · Eun Sun Lee¹ · Ara Ko¹ · Hyun Jeong Park¹ · Sung Bin Park¹ · Byung Ihn Choi¹ · Young Youn Cho² · Stephan Kannengiesser³

Received: 10 May 2019 / Revised: 1 September 2019 / Accepted: 2 October 2019
© European Society of Radiology 2019

Abstract

Objectives To determine the technical success rates of MR elastography (MRE) according to established gradient-recalled echo (GRE) and spin-echo echo-planar imaging (SE-EPI) sequences and to compare liver stiffness (LS) values between the sequences during expiratory and inspiratory phases in patients with chronic liver disease or liver cirrhosis.

Methods One hundred and eight patients who underwent MRE were included in this retrospective study. MRE was performed at 3 T based on both sequences during expiration as well as inspiration. Technical failure of MRE was determined if there was no pixel value with a confidence index higher than 95% and/or no apparent shear waves imaged. LS measurements were performed using free-drawing region of interest. To evaluate clinical factors related to the technical success rate of MRE, we assessed etiology of liver disease, ascites, body habitus, iron deposition, and liver morphology of patients. Statistical analysis was performed with the Wilcoxon test, Bland-Altman plot, independent *t* test, Mann-Whitney test, and McNemar test.

Results The technical success rate of MRE in SE-EPI was significantly higher than that of GRE (98.1% vs. 80.7%, $p < 0.0001$). On the basis of univariate analysis, height, weight, and BMI were significantly associated with failure of MRE ($p < 0.05$). There was no significant difference in LS values between GRE and SE-EPI (2.82 kPa vs. 2.92 kPa ($p > 0.05$)). However, the LS values were significantly higher during inspiration than expiration with both GRE and SE-EPI ($p < 0.0001$).

Conclusion MRE in SE-EPI during expiratory breath-hold can be used as a reliable examination to evaluate liver fibrosis.

Key Points

- The technical success rate of MR elastography in spin-echo echo-planar imaging (SE-EPI) was significantly higher than that in gradient-recalled echo (GRE) during both the inspiratory and expiratory phases.
- Liver stiffness values were significantly higher during inspiration than during expiration in both GRE and SE-EPI.
- MR elastography in SE-EPI during expiratory breath-hold can be used as a reliable examination in patients with liver fibrosis.

Keywords Liver cirrhosis · Magnetic resonance imaging · Elasticity imaging techniques · Echo-planar imaging · Diagnosis

✉ Eun Sun Lee
seraph377@cau.ac.kr

¹ Department of Radiology, Chung-Ang University Hospital, Chung-Ang University College of Medicine, 102, Heukseok-ro, Dongjak-gu, Seoul 06973, Republic of Korea

² Department of Internal Medicine, Chung-Ang University Hospital, Chung-Ang University College of Medicine, 102, Heukseok-ro, Dongjak-gu, Seoul 06973, Republic of Korea

³ Siemens Healthcare GmbH, Erlangen, Germany

Abbreviations

BMI	Body mass index
CI	Confidence interval
CLD	Chronic liver disease
CTP	Child-Turcotte-Pugh
GRE	Gradient-recalled echo
HBV	Hepatitis B virus
HCC	Hepatocellular carcinoma
HCV	Hepatitis C virus
kPa	Kilopascals
LC	Liver cirrhosis

LS	Liver stiffness
MRE	Magnetic resonance elastography
ROI	Region of interest
SE-EPI	Spin-echo echo-planar imaging
TE	Transient elastography

Introduction

Liver fibrosis is characterized by excessive deposition of the extracellular matrix, leading to consequent liver architectural distortion [1]. As progressive liver fibrosis leads to cirrhosis, it is associated with potential complications, such as liver failure, portal hypertension, varices, hepatocellular carcinoma (HCC), and hepatic encephalopathy [2, 3]. However, hepatic fibrosis is no longer considered an irreversible process due to the substantial recent development of anti-fibrotic therapies [4, 5]. Therefore, early diagnosis of cirrhosis and accurate measurement of the degree of fibrosis is important to determine the appropriate treatment and prognosis [6].

Percutaneous liver biopsy has been considered the standard for evaluating liver fibrosis, but it has several limitations, including poor patient compliance, invasiveness, risks of complication, sampling errors, and inter-observer variability in interpretation [1, 3, 7]. For these reasons, there have been many attempts to evaluate the degree of liver fibrosis with noninvasive options, including the use of serum markers, transient elastography (TE), and magnetic resonance elastography (MRE) [2, 3]. Among these techniques, MRE is considered to be the best method for measuring the degree of liver fibrosis because of its high accuracy and reproducibility with a large sample volume [3, 8, 9]. Technically, MRE is based on a phase contrast imaging method that images mechanical wave propagation and assesses tissue stiffness [2]. Using MRE, the degree of liver stiffness (LS) can be objectively measured and quantified in kilopascals (kPa) [9].

Until recently, the gradient-recalled echo (GRE)–sequence-based MRE has been most commonly used [10], and it has been well-validated by many previous studies for liver fibrosis evaluation [1, 2, 11]. However, in the iron-overload liver, GRE-MRE is known to exhibit high technical failure rate, as the sequence is sensitive to the short T2* transverse relaxation time [11, 12]. Considering that iron-overloading is not unusual in chronic liver disease (CLD) [13], this drawback of GRE-MRE could be critical. On the contrary, a spin-echo echo-planar imaging (SE-EPI) sequence for MRE, commercially available for nearly a decade on some but not all 3.0 T MRI systems, has been shown to be less sensitive to transverse relaxation signal decay [14, 15], resulting in fewer technical failures due to susceptibility [10–12]. In addition, SE-EPI-MRE has been considered to provide better estimates of stiffness maps for increased spatial coverage and larger areas of stiffness measurement, resulting in a lower overall technical

failure rate [2, 11]. Another technical concern regarding MRE is the respiratory effect. Conventionally, MRE has been performed during the end-expiration period with a breath-hold because increased portal flow during inspiration has been believed to have a theoretical effect on LS [16], and it is known that the measurement variability and hepatic positional changes between breath-holds can be minimized at end-expiration rather than at end-inspiration [17, 18].

However, to the best of our knowledge, there is no published study that compares the technical failure rates of GRE-MRE and SE-EPI-MRE as well as the LS values obtained during inspiration and expiration in the same patient with a large study population.

Therefore, the purpose of our study was to determine the technical success rates of MRE according to established GRE and SE-EPI sequences in the same study population comprising patients with CLD or liver cirrhosis (LC). An additional objective was to compare LS values between GRE-MRE and SE-EPI-MRE during inspiratory and expiratory phases.

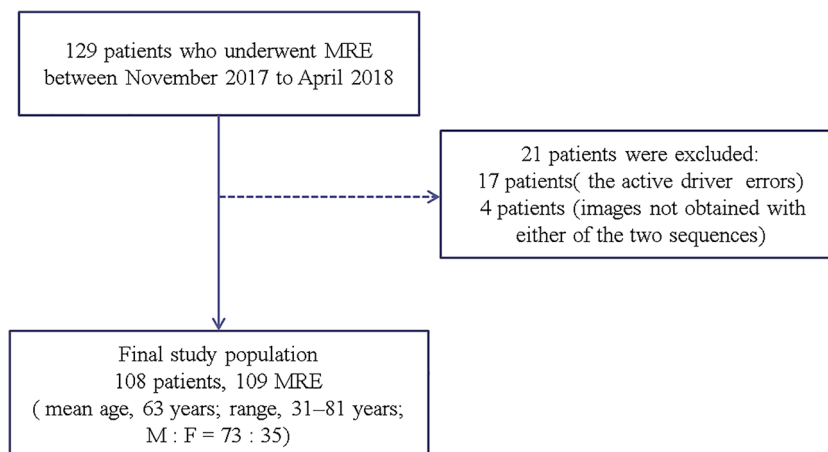
Materials and methods

Patients

Our local institutional review board approved this study. Between November 2017 and April 2018, 129 patients underwent MRE at our hospital. Of those, 17 patients were excluded from the study due to active driver errors; patients with images not obtained with either of the two sequences were also excluded ($n = 4$). Thus, a total of 108 patients (mean age, 63 years; range, 31–81 years; M:F = 73:35) were included in this retrospective study (Fig. 1). MRE was performed at 3 T based using standard GRE and prototype SE-EPI sequences during expiration and inspiration. MRE is part of the routine liver MRI protocol at our institution. The indications for liver MRI were as follows: HCC screening/surveillance, other malignant lesions (including metastases), focal liver lesions, and others.

MRI and MRE acquisition

All MR examinations were performed on a 3-T MR unit (MAGNETOM Skyra, Siemens Healthcare) using the integrated spine matrix and body matrix coils. The patients were examined in the supine position, and the receiver coil was positioned to cover the upper abdomen. Patients underwent a routine clinical imaging protocol of the liver before and after the injection of a contrast agent (gadoteric acid, Primovist; Bayer Healthcare), which included the following sequences: breath-hold axial and coronal T2-weighted half-Fourier acquisition single-shot fast spin-echo, axial in- and opposed-phase chemical shift imaging, breath-hold T2-weighted fast spin-

Fig. 1 Flow diagram of the final study population

echo with fat suppression, axial diffusion-weighted imaging, and axial 3D fat-suppressed T1-weighted imaging.

Liver MRE sequences were performed before the administration of the contrast agent. For MRE wave generation, a 19-cm-diameter passive acoustic driver was placed on the right side of the abdomen at the level of the xiphoid process. Then,

using the active driver (Resoundant), 60 Hz shear wave propagation was induced in the liver by delivering continuous acoustic vibration through a flexible vinyl tube to the passive driver. For the GRE sequence, a total of four slices were acquired in four consecutive breath-holds at end-expiration and end-inhalation phases, respectively. The acquisition time was

Table 1 Characteristics of the study population

Total ($n = 109$)			
Patient characteristics			
Age (mean years (range))		63 (31–81)	
Sex (male/female)		73/109 (67%/36/109 (33%))	
Indications for MRE			
HCC screening/surveillance		79/109 (73.1%)	
Other malignant lesions		18/109 (16.5%)	
Benign focal liver lesions		8/109 (7.3%)	
Others		4/109 (3.6%)	
LC, 79/109 (73.1%)		Non-LC, 30/109 (26.9%)	
CTP A	67/79 (84.8%)	CLD	12/30 (40%)
B	8/79 (10.1%)	Normal liver	18/30 (60%)
C	4/79 (5.1%)		
Etiologies of liver disease, 91/109 (83.5%)			Normal liver, 18/109 (16.5%)
HBV	48/91 (52.7%)		
HCV	7/91 (7.6%)		
Alcohol abuse	17/91 (18.6%)		
Autoimmune	1/91 (1.1%)		
Other	18/91 (19.7%)		
Iron deposition			
Technical error		7/109 (6.4%)	
R2* value < 115 s ⁻¹		102/109 (93.5%)	
Ascites			
None		92/109 (84.4%)	
Scanty		13/109 (11.9%)	
Moderate		1/109 (0.9%)	
Massive		3/109 (2.7%)	

HCC hepatocellular carcinoma, CTP Child-Turcotte-Pugh, CLD chronic liver disease, HBV hepatitis B virus, HCV hepatitis C virus, LC liver cirrhosis

Table 2 Technical success rate of MRE based on the sequence

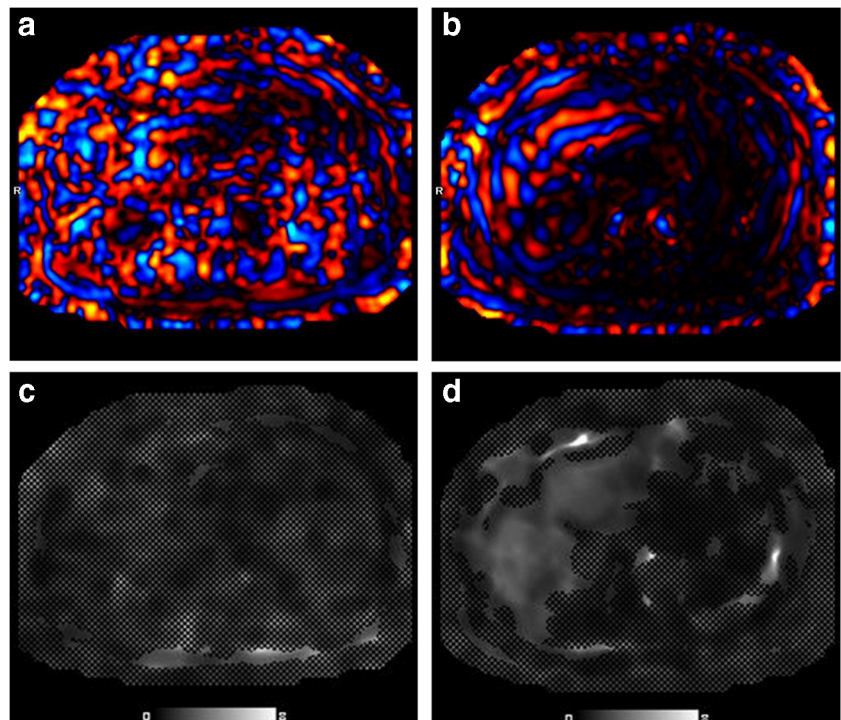
	SE-EPI	GRE	
Inspiration	107/109 (98.1%)	84/109 (77.1%)	$p < 0.0001$
Expiration	107/109 (98.1%)	88/109 (80.7%)	

The technical success rate of MRE was significantly higher in SE-EPI than in GRE

GRE gradient-recalled echo, SE-EPI spin-echo echo-planar imaging

76 s, split into four breath-holds. The measurement parameters for the GRE-MRE sequence were as follows: repetition time/echo time, 50/23.75 ms; flip angle, 25°; field of view, 380 × 226; matrix size, 128 × 76; band width, 260 Hz/pixel; thickness, 5 mm; and inter-slice gap, 10 mm. For the prototype SE-EPI sequence, all four slices were acquired in a single breath-hold at the end-expiration and end-inhalation phases, respectively. The acquisition time was 11 s, during a single breath-hold. The measurement parameters for the SE-EPI-MRE sequence were as follows: repetition time/echo time, 1000/47 ms; flip angle, 90°; field of view, 380 × 380; matrix size, 100 × 100; band width, 2380 Hz/pixel; thickness, 6 mm; and inter-slice gap, 12 mm. When the acquisition was complete, the wave images were automatically processed by the MR scanner, and images were created that delineated the tissue stiffness (elastogram). These images represented relative shear stiffness in kPa and were expressed in a gray scale or color scale. In addition, the processing algorithm provided “confidence” maps as a measure of reliability of the stiffness estimation as well as elastograms where values with a corresponding confidence value below 95% were marked.

Fig. 2 A 56-year-old man with HBV cirrhosis. **a** MRE acquired using a two-dimensional GRE sequence at expiratory breath-hold; the shear wave pattern is irregular and bizarre, likely indicating technical failure. **b** MRE acquired using a two-dimensional SE-EPI sequence at expiratory breath-hold; the shear wave is well stratified and shows regular intervals between each wave, indicating technical success. Additionally, there is no pixel value with a confidence index higher than 95% in **c** when compared with **d**. HBV hepatitis B virus, GRE gradient-recalled echo, SE-EPI spin-echo echo-planar imaging, LS liver stiffness



Analysis of MR elastography and assessment of failure

Two radiologists (S.C. and A.K. with 2-year resident in training) independently analyzed the MRE data. Technical failure of an MRE was determined if there was no pixel value with a confidence index higher than 95% and/or no apparent shear waves were imaged [11]. LS measurements were performed using free-drawing regions of interest (ROI) by two observers in consensus for each data set, avoiding large vessels and solitary occupying lesion in the liver. Four liver MRE slices were obtained in one sequence. Thus, a total of 16 ROI values could be obtained if all sequences were successful in both GRE and SE-EPI during the inspiratory and expiratory periods. Technical failure was considered when none of the four ROI values were obtained from one sequence. Additionally, the reliable area without cross stripes was measured.

Factors of MRE failure

For the evaluation of clinical factors related to the technical success rate of an MRE, we assessed the etiology of the liver disease, presence of ascites, iron deposition, height, weight, body mass index (BMI), and liver morphology (cirrhosis vs. non-cirrhosis). If a patient had LC, we assessed the Child-Turcotte-Pugh (CTP) score. For the evaluation of ascites, the amount of ascites was graded on a scale between 0 and 3, as follows: 0, none; 1, scanty; 2, moderate; and 3, massive amount of ascites. Iron deposition was assessed using region of interest placements with $R2^*(1/T2^*)$ imaging, avoiding

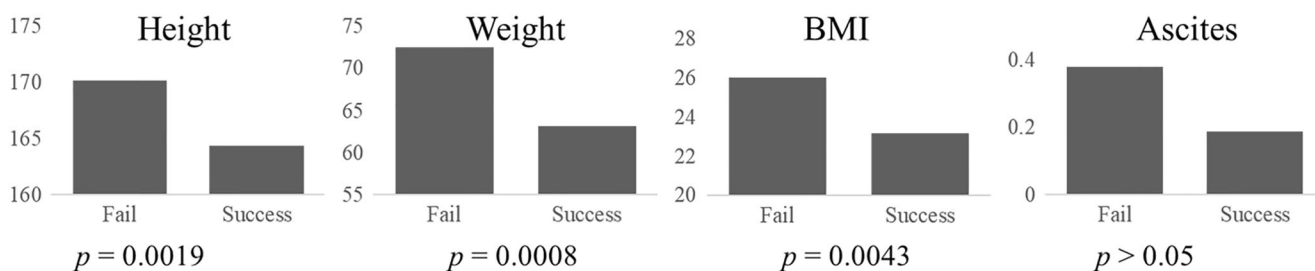


Fig. 3 Graphs showing that height, weight, and BMI are significantly associated with MRE failure (acquired with two-dimensional GRE sequence at expiratory breath-hold). BMI body mass index, GRE gradient-recalled echo

large vessels and solitary occupying lesions in the liver. The mean value was obtained from the values of three circular ROIs. An $R2^*$ value of 115 s^{-1} or more was defined as a significant increase in iron deposition [19].

Statistical analysis

The results are presented as median values for quantitative data. Median LS values between SE-EPI and GRE-MRE in the same patients were compared using the Wilcoxon signed rank test (paired samples Wilcoxon test) for both inspiration and expiration periods. In addition, the Bland-Altman plot was used to prove that there was no significant LS value difference between SE-EPI and GRE-MRE when the breathing period is the same. The significant parameters in the univariate analysis were assessed with the independent t test and Mann-Whitney test, depending on the parametric or nonparametric method. The technical success rates of MRE in SE-EPI and GRE were analyzed using McNemar's test. All analyses were performed using the commercially available statistical software MedCalc® (version 18.6). A two-sided p value of less than 0.05 was considered statistically significant.

Results

Patient characteristics

Because one patient underwent MRE measurements repeatedly, a total of 109 MRE examinations were assessed in this

study. The indications for liver MR imaging included HCC evaluation or follow-up ($n = 79$; 73.1%), other malignant lesions including metastases ($n = 18$; 16.5%), focal liver lesions ($n = 8$; 7.3%), and others ($n = 4$; 3.6%). None of these patients showed significant iron deposition: $R2^*$ value $< 115 \text{ s}^{-1}$ ($n = 102$; 93.5%) and technical error ($n = 7$; 6.4%). Among the included study patients, 79 patients had LC, 12 patients showed CLD configuration, and 18 patients showed normal liver configuration. The majority of the included patients had no ascites ($n = 92$), whereas the others presented with the following degrees of ascites: scanty ($n = 13$), moderate ($n = 1$), and massive ($n = 3$). The etiologies of liver disease were as follows: hepatitis B virus (HBV), hepatitis C virus (HCV), alcohol abuse, autoimmune, and others. Details are shown in Table 1.

Failure rate and factors of MRE failure

The technical success rate of MRE in SE-EPI was significantly higher than that in GRE during both the inspiratory and expiratory phases: 98.1% (SE-EPI_inspiration (IN)) vs. 77.1% (GRE_IN) and 98.1% (SE-EPI_expiration (EX)) vs. 80.7% (GRE_EX), $p < 0.0001$) (Table 2 and Fig. 2). On the basis of univariate analysis, the parameters height, weight, and BMI were significantly associated with MRE failure ($p < 0.05$). According to the multivariate analysis, only height was a significant independent factor ($p = 0.0312$). The mean value of ascites was higher in the failure group than in the success group, but this result was not statistically significant (0.38 vs. 0.19, $p = 0.29$) (Fig. 3). The failure rates according to

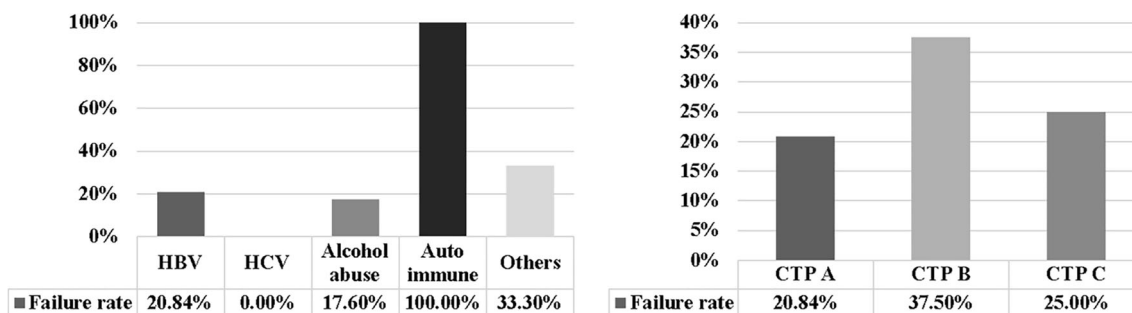


Fig. 4 Graphs showing the distributions of the MRE failure rates (acquired with two-dimensional GRE sequence at expiratory breath-hold) in relation to the etiology of the liver disease or the CTP score. GRE gradient-recalled echo, CTP Child-Turcotte-Pugh

Table 3 LS values, GRE vs. SE-EPI

	GRE	SE-EPI	
Inspiration	3.02 kPa (95% CI, 2.65–3.41)	3.03 kPa (2.94–3.19)	$p = 0.5250$
Expiration	2.82 kPa (2.49–3.16)	2.92 kPa (2.71–3.20)	$p = 0.1942$

There was no significant difference in LS values between GRE and SE-EPI

GRE gradient-recalled echo, SE-EPI spin-echo echo-planar imaging, LS liver stiffness, CI confidence interval

etiology were as follows: HBV (20.8%; 10 of 48), alcohol (17.6%; 3 of 17), autoimmune (100.0%; 1 of 1), and others (33.3%; 6 of 18); there was no failure detected in the HCV etiology group. Among the patients with LC ($n = 79$), the CTP scores were categorized as class A ($n = 67$), class B ($n = 8$), and class C ($n = 4$). The failure rates, according to these CTP score, were as follows: CTP A (20.8%; 14 of 67), CTP B (37.5%; 3 of 8), and CTP C (25.0%; 1 of 4) (Fig. 4). The technical success rate of MRE in the non-LC group was higher than that of the LC group in all sequences, including both inspiratory and expiratory phases; the results were as follows: non-LC vs. LC group, SE-EPI_IN (100%; (30 of 30) vs. 97.4%; (77 of 79)), SE-EPI_EX (100%; (30 of 30) vs. 97.4%; (77 of 79)), GRE_IN (83.3%; (25 of 30) vs. 74.6%; (59 of 79)), and GRE_EX (90%; (27 of 30) vs. 77.2%; (61 of 79)).

GRE vs. SE-EPI and inspiration vs. expiration

There was no significant difference in the LS values between GRE and SE-EPI during both inspiration and expiration: GRE_IN (3.02, (2.65–3.41, 95% confidence intervals (CIs)) kPa) vs. SE-EPI_IN (3.03 (2.94–3.19) kPa), and GRE_EX

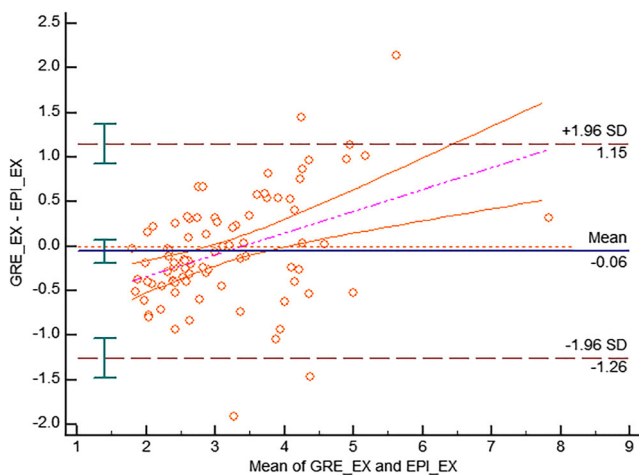


Fig. 5 The Bland-Altman plot for GRE_EX and SE-EPI_EX shows that there is no significant difference in LS values between GRE and SE-EPI during expiration (most of the scattered dots are within the error range). GRE gradient-recalled echo, SE-EPI spin-echo echo-planar imaging, IN inspiration, EX expiration

Table 4 LS values, inspiration vs. expiration

	Inspiration	Expiration	
GRE	3.02 kPa (95% CI, 2.65–3.41)	2.89 kPa (2.54–3.19)	$p = 0.0350$
SE-EPI	3.09 kPa (2.99–3.23)	2.94 kPa (2.75–3.18)	$p < 0.0001$

LS values were significantly higher during inspiration than during expiration

GRE gradient-recalled echo, SE-EPI spin-echo echo-planar imaging, LS liver stiffness, CI confidence interval

(2.82 (2.49–3.16) kPa) vs. SE-EPI_EX (2.92 (2.71–3.20) kPa) (Table 3 and Fig. 5). However, LS values were significantly higher during inspiration than expiration in both GRE and SE-EPI: GRE_IN (3.02, (2.65–3.41) kPa) vs. GRE_EX (2.89 (2.54–3.19) kPa) and SE-EPI_IN (3.09 (2.99–3.23) kPa) vs. SE-EPI_EX (2.94 (2.75–3.18) kPa) (Table 4). Additionally, the mean value of reliable area for measurement, without cross stripes, was significantly larger for the SE-EPI sequence: GRE_EX (1768.47 (1383.75–2158.61) mm²) vs. SE-EPI_EX (4665.66 (4294.68–4908.17) mm²), $p < 0.0001$) (Fig. 6).

Discussion

Our results show the advantages of a SE-EPI-MRE sequence in terms of technical success rate, image quality, and increased size of measurable image area according to the confidence value, with equivalent LS values, as compared with a standard GRE-MRE sequence. With increased ROI-size in the SE-EPI-MRE, the measured LS values would likely represent a more generalized assessment of the liver [11]. In addition, SE-EPI-MRE is less sensitive to transverse relaxation signal decay and shows more solid results than GRE-MRE, according to recent studies [2, 11, 12]. Furthermore, because of its shorter acquisition time [20], SE-EPI-MRE allows multiple slice acquisition in a single breath-hold, which results in increased liver coverage and a more tolerable experience for the patient. The clinical significance of our study findings is that SE-EPI sequences used in commercially available MRE implementations can be expected to provide better performance than GRE-MRE sequences—which have been validated in prior studies, in terms of good image quality, faster acquisition times, and high technical success rates. Our results are in agreement with prior studies [7, 11, 12, 21], in which SE-EPI-MRE showed a better subjective image quality, larger ROI-measurable area, and higher technical success rate compared with GRE-MRE.

In terms of factors related to technical failure, our study showed that height, weight, and BMI were significantly associated with MRE failure. These findings are consistent with those of previous studies in that high technical failure occurred

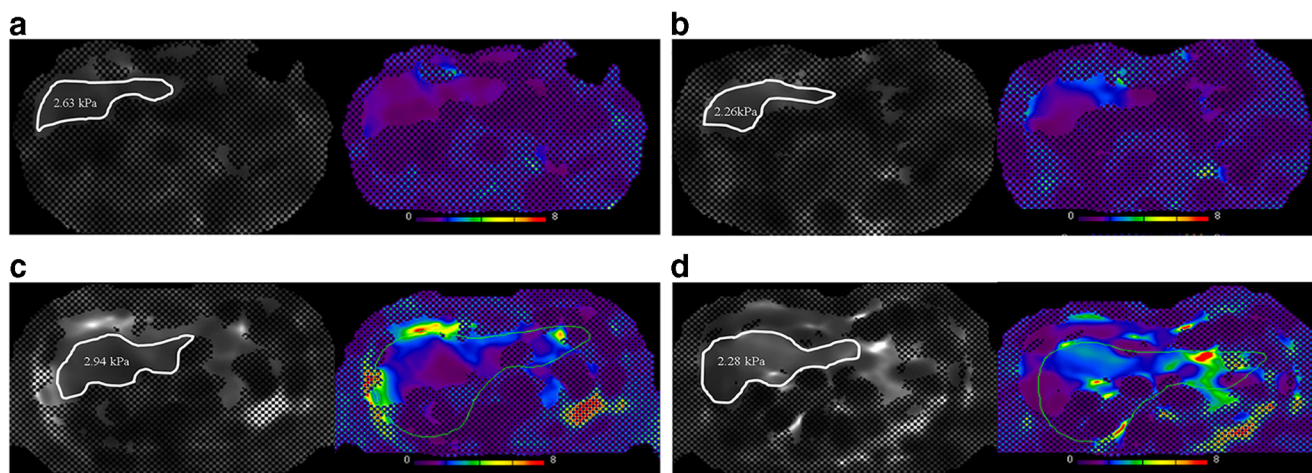


Fig. 6 A 32-year-old woman with a focal solid lesion in the liver (confirmed benign). MRE acquired using a two-dimensional GRE sequence during inspiratory (a) and expiratory (b) breath-holds. MRE acquired using a two-dimensional SE-EPI sequence during inspiratory (c) and expiratory (d) breath-holds. In both sequences, the LS values are

significantly higher during inspiration than expiration. Additionally, the reliable area for measurement, without cross stripes, is significantly larger with the SE-EPI sequence than with the GRE sequence, reflecting stability and reliability of the examination. GRE gradient-recalled echo, SE-EPI spin-echo echo-planar imaging, LS liver stiffness

in patient groups with high BMIs and weight [7]. It has been speculated that the fat tissue in obese people, disturbs the delivery of vibration from the generator to the liver [22]. However, in our study, the technical failure rate was higher in the taller group as well. Even though there is no established hypothesis, this result may be attributed to difficulty with placing the generator at an optimal location for taller patients. Unlike the results of a previous large population study [7], we found that the amount of ascites was not a predictive factor of liver MRE failure. However, there were only three patients with massive ascites in our study population; thus, determining the technical effect of ascites on MRE cannot be performed based on the results of our study. It is known that increased hepatic iron depositions lead to higher technical failure rates [10, 12]. However, no study patient exhibited significant iron accumulation. Therefore, it was not possible to evaluate the effect of iron deposition on MRE failure rate. The technical success rate of MRE in the non-LC group was higher than that in the LC group, which is in agreement with a previous large population study [7]; this may be because as the degree of cirrhosis increases, the liver architectural distortion becomes worse, making the propagation of vibration difficult. According to Pang et al [23], a higher liver stiffness value in TE is one of the determinants of poorly reliable liver stiffness measurements. Although this is a study using TE, the result is consistent with that in our study.

Conventionally, MRE has been performed during end-expiratory breath-hold, because increased portal flow during inspiration has been believed to affect LS [16]. Additionally, the measurement variability can be minimized at end-expiration [17]. However, to the best of our knowledge, there was only small population study ($n = 9$) [17] that investigated the effects of respiratory phases on MRE. In our study, the LS

values were significantly higher during inspiration than during expiration in both GRE and SE-EPI. According to Million et al [16], increased venous pressure due to congestive heart failure or the Valsalva maneuver strongly interferes with the liver stiffness measured with TE. Although this study examined the relationship between TE and respiration, the results are consistent with those of our study, in that increased portal flow affected the LS value.

This present study has several limitations. Firstly, the LS values obtained with MRE were not compared with other conventional methods, such as liver biopsy and TE; biopsy was not performed because of its invasiveness, and TE was only performed in a few cases. Secondly, the study population of patients with CLD was heterogeneous, owing to the retrospective nature of this study. Thirdly, all MRE examinations were performed using a single MR unit. Consequently, it would be difficult to generalize our study results to an actual clinical setting where various MR units and other parameters may be used. Lastly, the study population was not large enough to evaluate the performance of MRE for each etiologic cause and according to the CTP score or the degree of iron deposition. Therefore, a future prospective study using multiple MR units in a large patient population will be necessary.

In conclusion, the technical success rate of SE-EPI-MRE was significantly higher than that of GRE-MRE, but there was no significant difference in the LS values; however, these values were significantly higher during inspiration than expiration. Thus, MRE in SE-EPI during expiratory breath-hold can be used as a reliable examination in patients with liver fibrosis.

Funding information The authors state that this work has not received any funding.

Compliance with ethical standards

Guarantor The scientific guarantor of this publication is Eun Sun Lee.

Conflict of interest One of the authors (Stephan Kannengiesser) is an employee of Siemens Healthcare. The rest of the authors declare no relationships with any companies whose products or services may be related to the subject matter of the article.

Statistics and biometry No complex statistical methods were necessary for this paper.

Informed consent Written informed consent was waived by the Institutional Review Board.

Ethical approval Institutional Review Board approval was obtained.

Methodology

- Retrospective
- Diagnostic or prognostic study
- Performed at one institution

References

1. Kim YS, Jang YN, Song JS (2018) Comparison of gradient-recalled echo and spin-echo echo-planar imaging MR elastography in staging liver fibrosis: a meta-analysis. *Eur Radiol* 28:1709–1718
2. Venkatesh SK, Yin M, Ehman RL (2013) Magnetic resonance elastography of liver: technique, analysis, and clinical applications. *J Magn Reson Imaging* 37:544–555
3. Chang W, Lee JM, Yoon JH et al (2016) Liver fibrosis staging with MR elastography: comparison of diagnostic performance between patients with chronic hepatitis B and those with other etiologic causes. *Radiology* 280:88–97
4. Rockey DC (2008) Current and future anti-fibrotic therapies for chronic liver disease. *Clin Liver Dis* 12:939–962
5. Schuppan D, Ashfaq-Khan M, Yang AT, Kim YO (2018) Liver fibrosis: direct antifibrotic agents and targeted therapies. *Matrix Biol* 68:435–451
6. Gherlan GS (2015) Liver ultrasound elastography: more than staging the disease. *World J Hepatol* 7:1595
7. Wagner M, Corcuera-Solano I, Lo G et al (2017) Technical failure of MR elastography examinations of the liver: experience from a large single-center study. *Radiology* 284:401–412
8. Yoshimitsu K, Mitsufuji T, Shinagawa Y et al (2016) MR elastography of the liver at 3.0 T in diagnosing liver fibrosis grades: preliminary clinical experience. *Eur Radiol* 26:656–663
9. Venkatesh SK, Yin M, Ehman RL (2013) Magnetic resonance elastography of liver: clinical applications. *J Comput Assist Tomogr* 37:887
10. Cunha GM, Glaser KJ, Bergman A, Luz RP, De Figueiredo EH, Lobo Lopes FPP (2018) Feasibility and agreement of stiffness measurements using gradient-echo and spin-echo MR elastography sequences in unselected patients undergoing liver MRI. *Br J Radiol* 91:20180126
11. Wagner M, Besa C, Bou Ayache J et al (2016) MR Elastography of the liver: qualitative and quantitative comparison of gradient echo and spin echo echoplanar imaging sequences. *Invest Radiol* 51:575
12. Zhan C, Kannengiesser S, Chandarana H, Fenchel M, Ream J, Shanbhogue KP (2019) MR elastography of liver at 3 Tesla: comparison of gradient-recalled echo (GRE) and spin-echo (SE) echoplanar imaging (EPI) sequences and agreement across stiffness measurements. *Abdom Radiol (NY)* 44:1825–1833
13. Kowdley KV (2016) Iron overload in patients with chronic liver disease. *Gastroenterol Hepatol (NY)* 12:695–698
14. Huwart L, Salameh N, Ter Beek L et al (2008) MR elastography of liver fibrosis: preliminary results comparing spin-echo and echoplanar imaging. *Eur Radiol* 18:2535–2541
15. Garteiser P, Sahebjavaheer RS, Ter Beek LC et al (2013) Rapid acquisition of multifrequency, multislice and multidirectional MR elastography data with a fractionally encoded gradient echo sequence. *NMR Biomed* 26:1326–1335
16. Millonig G, Friedrich S, Adolf S et al (2009) Increased venous pressure increases liver stiffness (Fibroscan) independent of liver fibrosis. *Gastroenterology* 136:A–856
17. Wang K, Manning P, Szeverenyi N et al (2017) Repeatability and reproducibility of 2D and 3D hepatic MR elastography with rigid and flexible drivers at end-expiration and end-inspiration in healthy volunteers. *Abdom Radiol (NY)* 42:2843–2854
18. Kennedy P, Wagner M, Castéra L et al (2018) Quantitative elastography methods in liver disease: current evidence and future directions. *Radiology* 286:738–763
19. Kannengiesser S (2016) Iron quantification with LiverLab. *MAGNETOM Flash* 66:44–46
20. Serai SD, Dillman JR, Trout AT (2016) Spin-echo echo-planar imaging MR elastography versus gradient-echo MR elastography for assessment of liver stiffness in children and young adults suspected of having liver disease. *Radiology* 282:761–770
21. Kim YS, Song JS, Kannengiesser S, Seo SY (2017) Comparison of spin-echo echoplanar imaging and gradient recalled echo-based MR elastography at 3 Tesla with and without gadoxetic acid administration. *Eur Radiol* 27:4120–4128
22. Petta S, Di Marco V, Cammà C, Butera G, Cabibi D, Craxi A (2011) Reliability of liver stiffness measurement in non-alcoholic fatty liver disease: the effects of body mass index. *Aliment Pharmacol Ther* 33:1350–1360
23. Pang JX, Pradhan F, Zimmer S et al (2014) The feasibility and reliability of transient elastography using Fibroscan®: a practice audit of 2335 examinations. *Can J Gastroenterol Hepatol* 28:143–149

Publisher's note Springer Nature remains neutral with regard to jurisdictional claims in published maps and institutional affiliations.